Published in final edited form as:

Cereb Cortex. 2007 December ; 17(12): 2760–2768.

Quantitative Diffusion Tensor Tractography of Association and Projection Fibers in Normally Developing Children and Adolescents

Thomas J. Eluvathingal[1], **Khader M. Hasan**[1], **Larry Kramer**[1], **Jack M. Fletcher**[2], and **Linda Ewing-Cobbs**[3]

1 *Department of Diagnostic and Interventional Imaging, University of Texas Health Science Center at Houston, Houston, TX 77030, USA*

2 *Department of Psychology, University of Houston, Houston, TX 77204-5355, USA*

3 *Department of Pediatrics, University of Texas Health Science Center at Houston, Houston, TX 77030, USA*

Abstract

Whole-brain diffusion tensor tractography (DTT) at high signal-to-noise ratio and angular and spatial resolutions were utilized to study the effects of age, sex differences, and lateral asymmetries of 6 white matter pathways (arcuate fasciculus [AF], inferior longitudinal fasciculus, inferior fronto-occipital fasciculus [IFOF], uncinate fasciculus [UF], corticospinal tract [CST], and somatosensory pathway [SS]) in 31 right-handed children (6–17 years). Fractional anisotropy (FA), a measure of the orientational variance in water molecular diffusivity, and the magnitude of water diffusivity (parallel, perpendicular, and mean diffusivity) along the pathways were quantified. Three major patterns of maturation were observed: 1) significant increase in FA with age, accompanied by significant decreases in all 3 diffusivities (e.g., left IFOF); 2) significant decreases in all three diffusivities with age without significant changes in FA (e.g., left CST); and 3) no significant age-related changes in FA or diffusivity (e.g., SS). Sex differences were minimal. Many pathways showed lateral asymmetries. In the right hemisphere, the frontotemporal (FT) segment of AF was not visualized in a substantial (29%) number of participants. FA was higher in the left hemisphere in the FT segment of AF, UF, and CST, whereas it was lower in the frontoparietal segment of AF. This study provides normative data essential for the interpretation of pediatric brain DTT measurements in both health and disease.

Keywords

association and projection pathways; child and adolescent brain development; diffusion tensor tractography; hemispheric asymmetries

Address correspondence to Khader M. Hasan, PhD, Department of Diagnostic and Interventional Imaging, University of Texas Health Science Center at Houston, 6431 Fannin Street, MSB 2.100, Houston, TX 77030, USA. Email: khader.m.hasan@uth.tmc.edu..

This work is funded by National Institutes of Health grants R01-NS046308 awarded to L.E.-C., the National Institute of Child Health and Human Development P01-HD35946 awarded to J.M.F., and National Institute of Neurological Disorders and Stroke R01 NS052505 awarded to K.M.H. We wish to thank Vipul Kumar Patel for helping with data acquisition and Ambika Sankar for data management.

Supplementary Material

Supplementary material can be found at: http://www.cercor.oxfordjournals.org/.

Introduction

Magnetic resonance imaging (MRI) continues to play a major role in enriching our understanding of the dynamic structural and functional changes in the developing human brain. Longitudinal studies using MRI volumetric analysis and dynamic cortical mapping in youth aged 4–21 years show that gray matter density increases first in primary sensorimotor cortices and in frontal and occipital poles (Giedd et al. 1999; Gogtay et al. 2004; Lenroot and Giedd 2006). The remaining regions mature from back to front in parietal-to-frontal regions, with the association areas of the superior temporal and dorsolateral prefrontal cortices developing last (Giedd et al. 1999; Volpe 2000; Gogtay et al. 2004; Lenroot and Giedd 2006). From ages 5–11 years, dendritic arborization and pruning result in gray matter thinning in the right dorsal frontal and biparietal regions, in conjunction with increased gray matter in the left frontal and temporal-parietal language areas (Sowell et al. 2003). Nonlinear increases in gray matter peak in different regions, with increases in the frontal and parietal regions at about age 12 and in the temporal lobe at about age 16, followed by gray matter loss. Both postmortem histological (Yakovlev and LeCours 1967; Huttenlocher 1990) and MRI studies noted that white matter increases in a more linear pattern in frontal, temporal, and parietal regions. The protracted development of white matter appears to be related to myelination and is noted up to the third decade in adulthood (Sowell et al. 2003; Lenroot and Giedd 2006; Toga et al. 2006; Hasan et al. 2007). Previous MRI studies have demonstrated sex differences and lateral asymmetries in the global/regional brain gray matter volume/white matter volume/cortical thickness (De Bellis et al. 2001; Durston et al. 2001; Allen et al. 2003; Luders et al. 2005, 2006; for extensive review see Lenroot and Giedd 2006). Volumetric studies completed in children aged 4–18 years identified different ages of peak cortical and subcortical gray matter volumes in males and females; white matter increases in a more linear fashion (Lenroot and Giedd 2006). Diffusion tensor MRI quantitative region-of-interest (ROI) and voxel-based studies have also demonstrated sex differences and lateral asymmetries in the adult population (Peled et al. 1998; Kubicki et al. 2002; Szeszko et al. 2003; Park et al. 2004; Nucifora et al. 2005). However, the diffusion tensor imaging (DTI) literature addressing these issues in children aged 6–17 years is scant.

With the advent of diffusion tensor tractography (DTT), in vivo visualization of developmental changes in major compact pathways (or tracts) of the human brain is now possible (Conturo et al. 1999; Catani et al. 2002; Mori et al. 2002; Wakana et al. 2004; for reviews see Le Bihan et al. 2003; Mori and Zhang 2006). In addition to portraying the white matter changes associated with normal growth and development, DTI/DTT is also being extensively utilized to identify the white matter abnormalities underlying various neurocognitive/behavioral/psychiatric disorders in children (Neil et al. 1998; Klingberg et al. 2000; Barnea-Goraly et al. 2004, 2005; Nagy et al. 2004; Ashtari et al. 2005; Beaulieu et al. 2005; Berman et al. 2005; Partridge et al. 2005; Eluvathingal et al. 2006; Ewing-Cobbs et al. 2006; Hermoye et al. 2006; for reviews, Le Bihan et al. 2003; Hasan 2006; Mukherjee and McKinstry 2006). The lack of a quantitative normative database specific to white matter is a limiting factor in our understanding of brain development and the interplay with various pathologies (Crick and Jones 1993).

In most studies, DTI quantitative metrics have been obtained using either ROI analysis or voxel-based morphometry. A major limitation of ROI analysis is the possibility of error related to including other fiber tracts, or even gray matter and cerebrospinal fluid, along with white matter structures of interest (Snook et al. 2007). Voxel-based morphometry has the advantage of being observer independent and can be applied to study the whole brain. However, voxel-based morphometry also has some inherent shortcomings because of the requirements of spatial normalization and smoothing (Ashburner and Friston 2000; Jones et al. 2005). Both ROI and voxel-based morphometry methods have limited ability to quantify specific white matter pathways along their entire trajectories. DTT is a novel addition to the ROI and voxel-based

morphometry DTI methods that is capable of isolating specific pathways from adjacent gray matter, white matter, and cerebrospinal fluid and allows computation of the diffusion metrics specific to the entire tract of interest (Conturo et al. 1999; Catani et al. 2002; Mori et al. 2002; Wakana et al. 2004).

Studies using DTI to examine developmental changes in white matter microstructure have reported increases in fractional anisotropy (FA) and decreases in mean diffusivity with increasing age (Neil et al. 1998; McKinstry et al. 2002; Schmithorst et al. 2002; Schneider et al. 2004; Barnea-Goraly et al. 2005; Gupta et al. 2005; Dubois et al. 2006; Snook et al. 2007; for a review see Mukherjee and McKinstry 2006). FA is a measure of the intravoxel directionality of water translational random motion in presence of barriers and is expressed as a ratio ranging from 0 to 1 (0 = isotropic or no predilection for any particular direction and 1 = unidirectional). Mean diffusivity provides the overall magnitude of water diffusion (expressed in units of area per unit time or square millimeter per second) and is a sensitive indicator of maturational changes in the brain tissue (Pierpaoli et al. 1996; Mukherjee and McKinstry 2006). In addition, transverse diffusivity (the magnitude of water movement perpendicular to the long axis of axons) provides a more specific surrogate of changes associated with myelination, whereas axial diffusivity (the magnitude of water movement along the long axis of axons) is more related to the intrinsic characteristics of the axons or changes in the extraaxonal/extracellular space (Mukherjee et al. 2002; Song et al. 2005; Hasan and Narayana 2006; for a review see Beaulieu 2002).

To provide information regarding in vivo development of white matter, we examined developmental changes indexed by DTT in 4 association pathways: arcuate fasciculus (AF), inferior longitudinal fasciculus (ILF), inferior fronto-occipital fasciculus (IFOF), and uncinate fasciculus (UF) and 2 projection pathways: corticospinal tract (CST) and somatosensory pathway (SS). The above-mentioned association and projection pathways were selected due to their relatively large size, which increases the reliability of quantification. Furthermore, these tracts have been extensively studied using conventional MRI, morphometry, and DTT (Curnes et al. 1988; Makris et al. 1997; Catani et al. 2002, 2005; Mori et al. 2002, 2005; Wakana et al. 2004; Berman et al. 2005; Partridge et al. 2005; Dubois et al. 2006) and are also well described in the standard neuroanatomy text books and neuroanatomy atlases (Carpenter 1983; Mori et al. 2005; Schmahmann and Pandya 2006). Commissural or interhemispheric pathways and association pathways belonging to the limbic system (cingulum, fornix, and stria terminalis) were not included in the present study and will be the focus of a future work.

The AF has 3 distinct segments that interconnect cortical language centers located in the frontal, temporal, and parietal lobes of the left cerebral hemisphere (Dejerine 1895; Geschwind 1965; Catani et al. 2005; Makris et al. 2005; Schmahmann and Pandya 2006). The frontotemporal (FT) segment connects the inferior frontal cortex (known as Broca's area, in the dominant hemisphere) with superior temporal cortex (known as Wernicke's area in the dominant hemisphere). The frontoparietal (FP) segment connects inferior frontal cortex and parietal cortex. The temporoparietal (TP) segment connects the temporal cortex in the region of the superior and middle temporal gyri with the parietal cortex. The ILF connects the extrastriate occipital cortex with lateral temporal cortex, parahippocampal gyrus, and amygdala (Catani et al. 2002; Schmahmann and Pandya 2006), whereas IFOF connects the occipital lobe and frontal lobe. Anteriorly, the IFOF runs in close proximity with the UF and posteriorly with the ILF (Curran 1909; Catani et al. 2002; Kier et al. 2004; Schmahmann and Pandya 2006). The UF connects the anterior 3 temporal convolutions and the amygdala with gyrus rectus, medial retro-orbital cortex, and subcallosal area (Ebeling and Von Cramon 1992; Schmahmann and Pandya 2006). Regarding the projection pathways, the portion of CST studied in this work was restricted to the fibers originating from the precentral primary motor cortex (Brodmann area 4; Carpenter 1983). These fibers pass through the corona radiata, posterior limb of the

internal capsule, and cerebral peduncles to reach the medulla where they decussate at the level of the pyramids (Carpenter 1983). The SS studied extends from the level of the medial lemniscus to the postcentral somatosensory cortex (Brodmann areas 3, 2, and 1). Before reaching the postcentral cortex, fibers relay in the ventral posterolateral nucleus of the thalamus (Carpenter 1983).

In the present study, we utilized DTT in children aged 6–17 years to investigate for evidences in the white matter microstructure underlying the sex differences and lateral asymmetries in addition to our main goal of characterizing the effects of age. We examined the FA, mean, transverse, and axial diffusivities specific to the major association and projection pathways. A unique feature of this study was the DTT quantification of major pathways into subsegments (e.g., AF) to address the possibility that different segments of major pathways mature differently and even show differences related to sex and lateralization.

Materials and Methods

Participants

The 31 right-handed participants included 16 girls and 15 boys (age range, mean ± standard deviation = 6–17, 11.4 ± 3.1 years). The male and female groups did not differ in age (P = 0.63). All children were primarily English speaking, were identified as neurologically normal by review of medical history, and were medically stable at the time of the assessments. Each MRI scan was read as “normal” by a board-certified radiologist (L.K.). Written informed consent was obtained from the guardians and adolescents and assent from the children participating in these studies per the University of Texas Health Science Center at Houston institutional review board regulations for the protection of human research subjects.

MRI Data Acquisition

We acquired whole-brain data using a Philips 3.0 T Intera system with a SENSE parallel image receiving head coil. The MRI protocol included 1) 3D spoiled gradient echo, field of view = 240 × 240 mm^2 (isotropic voxel size = 0.9375 mm); 2) 2D dual spin-echo images TE_1/TE_2/TR = 10/90/5000 ms, in the axial plane (3 mm slice thickness, field of view = 240 × 240 mm^2 at 44 axial contiguous sections); and 3) phase-sensitive MRI in the sagittal and axial planes, in addition to a matching prescription of axial diffusion-encoded data as described below. The diffusion-weighted data were acquired using a single-shot, spin-echo diffusion-sensitized echo-planar imaging (EPI) sequence with the balanced *Icosa21*-encoding scheme (Hasan and Narayana 2003, 2006; Hasan 2006), a diffusion sensitization of b = 1000 s mm^{-2}, and repetition and echo times of TR = 6100 ms and TE = 84 ms, respectively. Echo planar imaging distortion artifacts were reduced by using a SENSE acceleration factor (R) or k-space under sampling equal to 2 (i.e., R = 2) (Bammer et al. 2002; Jaermann et al. 2004; Hasan and Narayana 2006). The slice thickness was 3 mm with 44 axial slices covering the entire brain (foramen magnum to vertex), a square field of view = 240 × 240 mm^2, and an image matrix of 256 × 256 that matched the 3D spoiled gradient echo and the 2D conventional MRI dual-fast spin-echo sequences. The number of nondiffusion-weighted or $b \sim 0$ magnitude image averages was 8; in addition, each encoding was repeated twice and magnitude averaged to enhance the signal-to-noise ratio (SNR) (Conturo et al. 1995). Thus, effectively 50 images were acquired for each of the 44 axial sections to cover the entire brain. The total DTI acquisition time was approximately 7 min and resulted in SNR-independent DTI metric estimation (Hasan et al. 2007).

Diffusion Tensor Tractography

After data preparation using in-house-developed procedures (Hasan 2006), compact fiber tracking was performed using DTI Studio software (H. Jiang and S. Mori, Johns Hopkins

University, Baltimore, MD; http://cmrm.med.jhmi.edu). Fiber tracking was based on the Fiber Assignment by Continuous Tracking algorithm with an FA threshold of 0.15 (except for the ILF and IFOF tracts for which it was 0.20) and angle threshold 60° (50° for ILF and IFOF). Brute-force fiber tractography and multiple ROI techniques were utilized to track the pathways of interest (Conturo et al. 1999; Mori et al. 1999; Huang et al. 2004; Wakana et al. 2004; Jiang et al. 2006). Once a fiber tract was reconstructed, the entire trajectory was verified on a slice-by-slice basis to ensure consistency with established anatomical landmarks (Carpenter 1983; Filley 2001; Schmahmann and Pandya 2006) as well as the DTT-based atlas of fiber pathways of human brain (Mori et al. 2005). In situations where a particular tract showed some unexpected connectivity or if there was a deviation relative to the known landmarks, the tract was excluded from further analyses. The mean FA and mean diffusivity were calculated from the individual values obtained from all the voxels that contained the fiber tract. The transverse and axial diffusivities were calculated as described elsewhere (Hasan and Narayana 2006). All the above-described pathways were separated with minor modifications to the traditional DTT methods described in the past (Catani et al. 2002, 2005; Mori et al. 2002, 2005; Wakana et al. 2004; see also supplementary file for more details on the fiber-tracking methods). The diffusion metrics were quantified for each of the individual tracts bilaterally (see Fig. 1 for examples of reconstructed fiber tracts).

Reliability of Fiber Tracking

An investigator (T.J.E.) who has established excellent intra- and interrater reproducibility for DTT in pediatric populations (Eluvathingal et al. 2006) evaluated the entire data sets. Intrarater reproducibility was tested by repeating all the measurements for the UF and AF in both hemispheres. These tracts were chosen as they have the most curved trajectory among all the fiber tracts studied. The results of the 2 measurements were analyzed using the paired Student's *t*-test, Pearson product-moment correlations, and Bland-Altman bias analyses (Bland and Altman, 1986). The Bland-Altman bias analysis procedure is based on plotting the mean versus the difference between 2 measurements in order to detect the baseline bias and other trends that the simple correlation fails to detect (Bland and Altman 1986).

Statistical Analyses

The effect of age on the measured FA, mean diffusion, and transverse and axial diffusivities on both the right and left hemispheres was examined individually using Pearson correlations and linear regression. Sex differences were examined using unpaired *t*-test and analysis of variance (ANOVA). Hemispheric differences in the diffusion metrics associated with individual fiber tracts were examined using the paired Student's *t*-test and ANOVA. All statistical analyses were conducted using the statistical toolbox in Matlab (Version 6.1; The Mathworks Inc., Natick, MA).

Results

All data sets included in the current study were free of image and subject motion artifacts. The intrarater reproducibility for fiber tracking was excellent for both UF and AF bilaterally. Neither the Bland-Altman bias analysis (UF right: $P = 0.94$, UF left: $P = 0.53$, AF right: $P = 0.10$, and AF left: $P = 0.56$) nor the *t*-test (UF right: $P = 0.76$, UF left: $P = 0.21$, AF right: $P = 0.51$, AF left: $P = 0.22$) showed any significant differences between the 2 measurements for UF and AF bilaterally. Correlations were very high between the 2 measurements (UF right: $r = 0.99$, UF left: $r = 0.99$, AF right: $r = 0.93$, and AF left: $r = 0.99$). Participants in whom fiber tracking failed or produced results inconsistent with the known course of particular tracts were excluded from further analyses. Table 1 details the number of participants included in the final analyses for each fiber tract. The descriptive and inferential statistics for the FA and mean

diffusivity measurements and correlations with age are given in Table 2 while transverse and axial diffusivities are given in Table 3.

Effects of Age

Table 2 shows that FA increased significantly with age in the following tracts: FP segment of right AF, right CST, left ILF, left IFOF, and bilateral UF. Although the other tracts studied showed a positive correlation of FA with age ($r = 0.08–0.38$), none attained statistical significance (see Table 2).

Table 3 shows that mean diffusivity decreased significantly with age in all the fiber tracts studied ($r = −0.39$ to $−0.69$), except in the SS, bilaterally. Transverse diffusivity followed the trends of mean diffusivity and decreased significantly with age in all tracts ($r = −0.41$ to $−0.67$), except ILF in the right hemisphere and SS, bilaterally (see Table 3). A significant decrease in axial diffusivity with increasing age ($r = −0.42$ to $−0.73$) was observed in most of the tracts studied, except for the right CST, ILF, and SS, bilaterally (see Table 3).

Sex Differences

A series of *t*-tests revealed few significant differences. Girls had significantly lower transverse diffusivity in the ILF bilaterally (right ILF: $P = 0.02$, left ILF: $P = 0.03$) and right IFOF ($P = 0.04$) compared with boys. The lower transverse diffusivity in the ILF was accompanied by lower mean diffusivity (right ILF: $P = 0.02$, left ILF: $P = 0.04$). There were no sex differences in FA or axial diffusivity in any tract.

Lateral Asymmetries

Laterality differences in the FA measurements were present for several tracts. Significantly higher FA in the left than right hemisphere was noted in the FT segment of AF ($P < 0.01$), CST ($P = 0.003$), and UF ($P < 0.03$). The ILF ($P = 0.07$) and IFOF ($P = 0.08$) demonstrated a trend toward higher FA in the left hemisphere. The FP segment of the AF was the only pathway that had significantly higher FA in the right than left hemisphere ($P = 0.001$). The remaining tracts, including the TP segment of AF pathway and the SS, did not show any laterality differences in FA (see supplementary Fig. 2).

Discussion

The present study utilized DTT and identified an increase in FA and a decrease in the axial, transverse, and mean diffusivities with age in most of the tracts studied. Consistent with previous reports (Schmithorst et al. 2002; Schneider et al. 2004; Barnea-Goraly et al. 2005), diffusivity measurements were more sensitive to age than FA (see Tables 2 and 3). In contrast, FA was more sensitive in detecting lateral asymmetries in the microstructure of various tracts. Lateral asymmetries in FA were obvious for AF, UF, and CST. We also noted minimal sex differences in the microstructure of tracts, especially IFOF in the right hemisphere and ILF, bilaterally. Despite technical differences with prior studies, the major findings of this study were generally consistent with earlier postmortem (Yakovlev 1967; Yakovlev and LeCours 1967; LaMantia and Rakic 1990), MRI volumetry (Giedd et al. 1999; Paus et al. 1999; Courchesne et al. 2000; Durston et al. 2001; Good et al. 2001; Matsuzawa et al. 2001; Sowell et al. 2003), and DTI reports (Mukherjee et al. 2001; McKinstry et al. 2002; Schmithorst et al. 2002; Schneider et al. 2004; Barnea-Goraly et al. 2005; Mukherjee and McKinstry 2006; Hasan et al. 2007; Snook et al. 2007) that show continued white matter maturation through childhood and adolescence. The lateral asymmetries observed were also consistent with previous reports (Yakovlev and Rakic 1966; Rademacher et al. 2001; Kubicki et al. 2002; Buchel et al. 2004; Park et al. 2004; Nucifora et al. 2005).

Effects of Age

Three age-related patterns were apparent in the FA and diffusivity. In the first pattern, a significant increase in FA with age was accompanied by significant decreases in all 3 diffusivities (FP segment of bilateral AF, left ILF, left IFOF, and bilateral UF, see Fig. 2*A*). It appears that increases in myelination (as measured by decreased transverse diffusivity) are accompanied by changes in the intrinsic characteristics of axons/changes in extraaxonal or extracellular space (as measured by decreased axial diffusivity) in these pathways. In the second pattern, there was a significant age-related decrease in the axial, transverse, and mean diffusivity measures that was not accompanied by a significant increase in FA (FT segment of left AF, bilateral TP segments of AF, right IFOF, and left CST; see Fig. 2*B*). Although this pattern may in part be attributable to progressive myelination, the commensurate changes in the axial diffusivities may also indicate continued changes in intrinsic characteristics of axons/changes in extraaxonal or extracellular space. In the third pattern, there were no significant age-related changes in FA or diffusivity (SS, see Fig. 2*C*). The right ILF and right CST did not fit into any of the 3 patterns.

The 3 patterns of microstructural changes detected by DTT may reflect a continuum representing different stages of white matter maturation. The pathways that exhibited the first pattern of maturation (FP segment of bilateral AF, left ILF, left IFOF, and bilateral uncinate) play an important role in higher cognitive functions (e.g., language, visuospatial processing, and attention; Carpenter 1983; Kandel et al. 1998; Filley 2001; Schmahmann and Pandya 2006). Children show rapid development of these functions for the age range included in this study (Behrman et al. 2000). In contrast, pathways that demonstrated the second pattern of maturation (FT segment of left AF [speech], left CST [voluntary/fine motor movements], and bilateral TP segments of AF [auditory spatial/audiovisual processing]) (Carpenter 1983; Kandel et al. 1998; Filley 2001; Schmahmann and Pandya 2006) likely undergo substantial maturation before the age of 6 years to support basic proficiency in speech, motor control, and auditory and visual skills that are necessary for the elaboration of higher cognitive skills (Behrman et al. 2000). The primary SS was the only one that showed the third pattern. Berman et al. (2005) reported an increase in FA and a decrease in diffusivity with age in both the CST and SS tracts in neonates. There was no difference in the effect of age between these 2 pathways (Berman et al. 2005). The present study demonstrated that in the age group of 6–17 years, only CST continued to show age-related changes and not the SS, implying an early maturation of SS compared with CST. From a functional point of view, children achieve these senses fairly quickly after birth (Behrman et al. 2000). The right CST and right ILF pathways did not fit into any of the above-discussed patterns. A possible explanation for this could be that these tracts are in a transitional phase of the above-mentioned 3 patterns. Right CST may be in a phase of transition from the second pattern to the third pattern, whereas for right ILF it was between the first and second.

Altogether, it appears that only a certain combination of changes in the transverse and axial diffusivities are able to produce a gross architectural change (Pierpaoli et al. 1996) adequate enough to be detected by the FA. Also, FA in a particular tract is influenced by the architectural changes in the surrounding tracts (Pierpaoli et al. 1996). The cross-sectional nature of the present study and relatively narrow age range and sample size limit further statistical analyses to evaluate the differences among these patterns, as well as how and when a particular tract changes from one pattern to the other.

Sex Differences

There were few effects of sex in the present study, the exception representing a significantly lower transverse diffusivity in the IFOF in the right hemisphere and ILF in both hemispheres of girls compared with boys. This finding may indicate higher myelin content in these tracts

in girls. Previous DTI studies in adults (Szeszko et al. 2003) also have reported microstructural evidence for sex differences. However, the technical differences and the differences in the age group studied make direct comparisons infeasible. MRI volumetric studies in the past have shown that sex differences are more pronounced in the white matter volume, and females are known to have higher gray matter to white matter ratios compared with males (Allen et al. 2003). Allen et al. (2003) proposed that this difference in gray matter to white matter ratio is mainly due to less white matter in females. The authors also speculated that women are likely compensating neuronally in some way for their relatively smaller cranial capacities. The present finding suggestive of higher myelin content in the IFOF in the right hemisphere and bilateral ILF may be due to such a neuronal compensation. Higher myelin thickness is known to be the most significant factor that makes neuronal transmission more efficient (Kandel et al. 1998). In view of our small sample, these results need to be reported in larger samples.

Lateral Asymmetries

The present study detected a leftward asymmetry (left > right) in FA in the FT segment of AF, UF, and CST. The only pathway that showed a rightward asymmetry (right > left) in FA was the FP segment of AF (see supplementary Fig. 2). Further detailed analysis of hemispheric differences in the rate of change of the diffusion metrics with age did not reveal any significant results except for a trend for higher rate of change of FA in the left IFOF compared with right ($P = 0.09$) and a higher rate of change in the transverse diffusivity in the right CST compared with left ($P = 0.08$).

Arcuate Fasciculus

The present study is the first DTT application to quantify the 3 segments of AF based on the lobar connectivity of individual components described by Catani et al. (2005). One of the major observations related to the AF was that the FT segment of the AF was not demonstrable in 29% (17/24) of participants (Fig. 1). A similar observation was also reported in a recent DTT study in right-handed young adults (Nucifora et al. 2005). We observed a higher FA in the FT segment of the left AF. Using a DTI-based, voxel-based morphometry study in right-handed adults, Buchel et al. (2004) also reported a higher FA in regions corresponding to the FT segment of left AF. However, exclusion of the participants who did not have a demonstrable FT segment on the right side (7 of 24 participants) resulted in no identification of hemispheric differences in the measured FA, which is expected as these were the participants who demonstrated maximum asymmetry. To account for this, a Kruskal–Wallis nonparametric test was performed that also showed a trend toward significantly higher FA ($P = 0.09$) in the left FT segment (see supplementary Fig. 2). The higher FA in the left than right FT segment is consistent with the well-known functional and anatomical lateralization of language to the dominant hemisphere (Broca 1861; Dejerine 1895; Geschwind 1965; Geschwind and Levitsky 1968). It is possible that the children in whom the right FT was absent or the FA in the right FT was low may have more striking language lateralization compared with children with more symmetrical measurements. Combined functional, structural, and diffusion tensor MRI studies correlating individual variations in language lateralization with individual variations in the structural anatomy and FA will be extremely useful in further understanding the issue of language lateralization, and many have implications for predicting language recovery from stroke, traumatic brain injury, and other neurological disorders.

In contrast to the leftward asymmetry of the FT segment of AF, the FP segment showed a significant rightward asymmetry in the FA. This finding is consistent with the findings of Buchel et al. (2004), who reported an area of significantly increased FA in the white matter underneath the right inferior parietal region, consistent with the course of the FP segment of AF. The higher FA in the present study was associated with higher mean and axial diffusivity. Differences in the degree of tortuosity (i.e., straightness) of individual axons in the voxels are

known to change the magnitude of the axial diffusivity that in turn can change the observed anisotropy (Takahashi et al. 2000). It may be that a less prominent or absent FT segment of AF on the right side may allow the FP segments to be straighter on the right side compared with the left, leading to the observed higher axial diffusivity and higher FA on right side.

Uncinate Fasciculus

To the best of our knowledge, there are no published quantitative DTT data on the asymmetry of the UF in the 6–17 years age group. Our finding of higher FA in left UF compared with right UF is consistent with previous reports in adults (Kubicki et al. 2002; Park et al. 2004). Using DTI-based, voxel-based morphometry and ROI analyses, Park et al. (2004) showed that the asymmetry in the measured FA of the UF depends on the region studied; the inferior portion showed a greater FA in the right hemisphere, whereas the superior portion showed a greater FA in the left hemisphere. The DTT methods used in the present study averaged the FA values obtained from all the voxels occupied by this tract. Because the UF has a shorter inferior segment and a longer superior segment, it is possible that the mean value is influenced by the longer superior portion, which was reflected by a leftward asymmetry in the present study. The higher FA observed in our study was not associated with any significant asymmetry in the diffusivities.

Corticospinal Tract

FA was higher in the left CST in 20 of 28 of the right-handed participants, whereas transverse diffusivity was lower in 21 of 28. Taken together, the significantly higher FA combined with lower transverse diffusivity is consistent with a conjecture of higher myelin content (Beaulieu 2002; Mukherjee et al. 2002; Song et al. 2005; Hasan and Narayana 2006) in the left CST. Our findings are consistent with previous postmortem reports by Yakovlev and Rakic (1966) as well as the more recent reports by Rademacher et al. (2001) on hemispheric asymmetries of CST. In addition, there is strong functional evidence that right-handed individuals exhibit hemispheric asymmetry favoring the left hemisphere in voluntary movements (Kawashima et al. 1993; Kim et al. 1993; Civardi et al. 2000).

Future Directions

Altogether, FA increased and the axial, transverse, and mean diffusivities decreased with age. The mean (12 of 16 tracts), transverse (12 of 16 tracts), and axial diffusivities (10 of 16 tracts) were comparable in sensitivity in detecting significant age-related changes. The FA was less sensitive (6 of 16 tracts) in detecting age-related changes, whereas it was more sensitive in identifying lateral asymmetries compared with any of the diffusivity measurements. Sex differences were minimal and were limited to the ILF and IFOF. The age-related changes are consistent with ongoing myelination (evidenced by a decrease in transverse diffusivity), along with changes in the extraaxonal/extracellular space/intraaxonal milieu (evidenced by decrease in axial diffusivity) in all the association pathways and CST. These findings are also consistent with previous reports on white matter maturation in this age group (Yakovlev 1967; Yakovlev and LeCours 1967; Giedd et al. 1999; Paus et al. 1999; Courchesne et al. 2000; Durston et al. 2001; Good et al. 2001; Matsuzawa et al. 2001; Mukherjee et al. 2001; McKinstry et al. 2002; Schmithorst et al. 2002; Sowell et al. 2003; Schneider et al. 2004; Barnea-Goraly et al. 2005; Lenroot and Giedd 2006; Snook et al. 2007). Due to the cross-sectional nature of the present study and the limited age range (6–17 years), we were not able to identify when and how these changes occur in a particular white matter pathway. Future extensions of this study should include larger male and female populations with a wider age range and additional statistical modeling of the interplay between microstructural DTI metrics and MRI volumetry (Hasan et al. 2007) and the accompanying cognitive and behavioral changes with development (Casey et al. 2005).

Supplementary Material

Refer to Web version on PubMed Central for supplementary material.

References

Allen JS, Damasio H, Grabowski TJ, Bruss J, Zhang W. Sexual dimorphism and asymmetries in the gray-white composition of the human cerebrum. Neuroimage 2003;18:880–894. [PubMed: 12725764]

Ashburner J, Friston KJ. Voxel-based morphometry—the methods. Neuroimage 2000;11:805–821. [PubMed: 10860804]

Ashtari M, Kumra S, Bhaskar SL, Clarke T, Thaden E, Cervellione KL, Rhinewine J, Kane JM, Adesman A, Milanaik R, et al. Attention-deficit/hyperactivity disorder: a preliminary diffusion tensor imaging study. Biol Psychiatry 2005;57:448–455. [PubMed: 15737658]

Bammer R, Auer M, Keeling SL, Augustin M, Stables LA, Prokesch RW, Stollberger R, Moseley ME, Fazekas F. Diffusion tensor imaging using single-shot ENSE-EPI. Magn Reson Med 2002;48:128–136. [PubMed: 12111940]

Barnea-Goraly N, Kwon H, Menon V, Eliez S, Lotspeich L, Reiss AL. White matter structure in autism: preliminary evidence from diffusion tensor imaging. Biol Psychiatry 2004;55:323–326. [PubMed: 14744477]

Barnea-Goraly N, Menon V, Eckert M, Tamm L, Bammer R, Karchemskiy A, Dant CC, Reiss AL. White matter development during childhood and adolescence: a cross-sectional diffusion tensor imaging study. Cereb Cortex 2005;15:1848–1854. [PubMed: 15758200]

Beaulieu C. The basis of anisotropic water diffusion in the nervous system—a technical review. NMR Biomed 2002;15:435–455. [PubMed: 12489094]

Beaulieu C, Plewes C, Paulson LA, Roy D, Snook L, Concha L, Phillips L. Imaging brain connectivity in children with diverse reading ability. Neuroimage 2005;25:1266–1271. [PubMed: 15850744]

Behrman, RE.; Kliegman, RM.; Jenson, HB. Nelson textbook of pediatrics. 16. W. B. Saunders; Philadelphia (PA): 2000.

Berman JI, Mukherjee P, Partridge SC, Miller SP, Ferriero DM, Barkovich AJ, Vigneron DB, Henry RG. Quantitative diffusion tensor MRI fiber tractography of sensorimotor white matter development in premature infants. Neuroimage 2005;27:862–871. [PubMed: 15978841]

Bland JM, Altman DG. Statistical methods for assessing agreement between two methods of clinical measurement. Lancet 1986;1:307–310. [PubMed: 2868172]

Broca P. Remarques sur la siegé de la faculté du langue. Bull Soc Anatom Paris 1861;6:330–357.

Buchel C, Raedler T, Sommer M, Sach M, Weiller C, Koch MA. White matter asymmetry in the human brain: a diffusion tensor MRI study. Cereb Cortex 2004;14:945–951. [PubMed: 15115737]

Carpenter, MB. Human neuroanatomy. 8. Baltimore (MD): Williams & Wilkins; 1983.

Casey BJ, Tottenham N, Liston C, Durston S. Imaging the developing brain: what have we learned about cognitive development? Trends Cogn Sci 2005;9:104–110. [PubMed: 15737818]review

Catani M, Howard RJ, Pajevic S, Jones DK. Virtual in vivo interactive dissection of white matter fasciculi in the human brain. Neuroimage 2002;17:77–94. [PubMed: 12482069]

Catani M, Jones DK, Ffytche DH. Perisylvian language networks of the human brain. Ann Neurol 2005;57:8–16. [PubMed: 15597383]

Civardi C, Cavalli A, Naldi P, Varrasi C, Cantello R. Hemispheric asymmetries of cortico-cortical connections in human hand motor areas. Clin Neurophysiol 2000;111:624–629. [PubMed: 10727913]

Conturo TE, Lori NF, Cull TS, Akbudak E, Snyder AZ, Shimony JS, McKinstry RC, Burton H, Raichle ME. Tracking neuronal fiber pathways in the living human brain. Proc Natl Acad Sci USA 1999;96:10422–10427. [PubMed: 10468624]

Conturo TE, McKinstry RC, Aronovitz JA, Neil JJ. Diffusion MRI: precision, accuracy and flow effects. NMR Biomed 1995;8:307–332. [PubMed: 8739269]

Courchesne E, Chisum HJ, Townsend J, Cowles A, Covington J, Egaas B, Harwood M, Hinds S, Press GA. Normal brain development and aging: quantitative analysis at in vivo MR imaging in healthy volunteers. Radiology 2000;216:672–682. [PubMed: 10966694]

Crick F, Jones E. Backwardness of human neuroanatomy. Nature 1993;361:109–110. [PubMed: 8421513]

Curnes JT, Burger PC, Djang WT, Boyko OB. MR imaging of compact white matter pathways. Am J Neuroradiol 1988;9:1061–1068. [PubMed: 3143230]

Curran EJ. A new association fiber tract in the cerebrum with remarks on the fiber tract dissection method of studying the brain. J Comp Neurol 1909;19:645–656.

De Bellis MD, Keshavan MS, Beers SR, Hall J, Frustaci K, Masalehdan A, Noll J, Boring AM. Sex differences in brain maturation during childhood and adolescence. Cereb Cortex 2001;11:552–557. [PubMed: 11375916]

Dejerine, J. Anatomie des centres nerveux. 1. Paris: Rueff et Cie; 1895.

Dubois J, Hertz-Pannier L, Dehaene-Lambertz G, Cointepas Y, Le Bihan. Assessment of the early organization and maturation of infants' cerebralwhite matter fiber bundles: a feasibility study using quantitative diffusion tensor imaging and tractography. Neuroimage 2006;30:1121–1132. [PubMed: 16413790]

Durston S, Hulshoff Pol HE, Casey BJ, Giedd JN, Buitelaar JK, van Engeland H. Anatomical MRI of the developing human brain: what have we learned? J Am Acad Child Adolesc Psychiatry 2001;40:1012–1020. [PubMed: 11556624]

Ebeling U, Von Cramon D. Topography of uncinate fascicle and adjacent temporal fiber tracts. Acta Neurochir 1992;115:143–148.

Eluvathingal TJ, Chugani HT, Behen ME, Juhasz C, Muzik O, Maqbool M, Chugani DC, Makki M. Abnormal brain connectivity in children after early severe socioemotional deprivation: a diffusion tensor imaging study. Pediatrics 2006;117:2093–2100. [PubMed: 16740852]

Ewing-Cobbs L, Hasan KM, Prasad MR, Kramer L, Bachevalier J. Corpus callosum diffusion anisotropy correlates with neuropsychological outcomes in twins disconcordant for traumatic brain injury. Am J Neuroradiol 2006;27:879–881. [PubMed: 16611782]

Filley, CM. The behavioral neurology of white matter. New York: Oxford; 2001.

Geschwind N. Disconnexion syndromes in animals and man. Brain 1965;88:237–294. [PubMed: 5318481]

Geschwind N, Levitsky W. Human brain left-right asymmetries in temporal speech region. Science 1968;161:186–187. [PubMed: 5657070]

Giedd JN, Blumenthal J, Jeffries NO, Rajapakse JC, Vaituzis AC, Liu H, Berry YC, Tobin M, Nelson J, Castellanos FX. Development of the human corpus callosum during childhood and adolescence: a longitudinal MRI study. Prog Neuro-psychopharmacol Biol Psychiatry 1999;23:571–588.

Gogtay N, Giedd JN, Lusk L, Hayashi KM, Greenstein D, Vaituzis AC, Nugent TF 3rd, Herman DH, Clasen LS, Toga AW, et al. Dynamic mapping of human cortical development during childhood through early adulthood. Proc Natl Acad Sci 2004;101:8174–8179. [PubMed: 15148381]

Good CD, Johnsrude IS, Ashburner J, Henson RN, Friston KJ, Frackowiak RS. A voxel-based morphometric study of ageing in 465 normal adult human brains. Neuroimage 2001;14:21–36. [PubMed: 11525331]

Gupta RK, Hasan KM, Trivedi R, Pradhan M, Das V, Parikh NA, Narayana PA. Diffusion tensor imaging of the developing human cerebrum. J Neurosci Res 2005;81:172–178. [PubMed: 15931676]

Hasan, KM. Fundamentals of diffusion tensor imaging of the entire human brain: review of basic theory, data acquisition, processing and potential applications at 1.5 T and 3.0 T. Chapter 1. In: Chen, FJ., editor. Progress in brain mapping research. Hauppauge (NY): Nova Science Publishers Inc; 2006. p. 1-80.

Hasan KM, Halphen C, Sankar A, Eluvathingal TJ, Kramer L, Stuebing KK, Ewing-Cobbs L, Fletcher JM. Diffusion tensor imaging-based tissue segmentation: Validation and application to the developing child and adolescent brain. Neuroimage 2007;34:1497–1505. [PubMed: 17166746]

Hasan KM, Narayana PA. Computation of the fractional anisotropy and mean diffusivity maps without tensor decoding and diagonalization: theoretical analysis and validation. Magn Reson Med 2003;50:589–598. [PubMed: 12939767]

Hasan KM, Narayana PA. Retrospective measurement of the diffusion tensor eigenvalues from diffusion anisotropy and mean diffusivity in DTI. Magn Reson Med 2006;56:130–137. [PubMed: 16755537]

Hermoye L, Saint-Martin C, Cosnard G, Lee SK, Kim J, Nassogne MC, Menten R, Clapuyt P, Donohue PK, Hua K, et al. Pediatric diffusion tensor imaging: normal database and observation of the white matter maturation in early childhood. Neuroimage 2006;29:493–504. [PubMed: 16194615]

Huang H, Zhang J, van Zijl PC, Mori S. Analysis of noise effects on DTI-based tractography using the brute-force and multi-ROI approach. Magn Reson Med 2004;52:559–565. [PubMed: 15334575]

Huttenlocher PR. Morphometric study of human cerebral cortex development. Neuropsychologia 1990;28:517–527. [PubMed: 2203993]

Jaermann T, Crelier G, Pruessmann KP, Golay X, Netsch T, Van Muiswinkel AM, Mori S, van Zijl PC, Valavanis A, Kollias S, et al. SENSE-DTI at 3 T. Magn Reson Med 2004;51:230–236. [PubMed: 14755645]

Jiang H, van Zijl PC, Kim J, Pearlson GD, Mori S. DtiStudio: resource program for diffusion tensor computation and fiber bundle tracking. Comput Methods Programs Biomed 2006;81:106–116. [PubMed: 16413083]

Jones DK, Symms MR, Cercignani M, Howard RJ. The effect of filter size on VBM analyses of DT-MRI data. Neuroimage 2005;26:546–554. [PubMed: 15907311]

Kandel, ER.; Schwartz, JH.; Jessel, TM. Essential of neural science and behavior. East Norwalk (CT): Appleton and Lange; 1998.

Kawashima R, Yamada K, Kinomura S, Yamaguchi T, Matsui H, Yoshioka S, Fukuda H. Regional blood flow changes of cortical motor areas and prefrontal areas in human related to ipsilateral and contralateral hand movement. Brain Res 1993;623:33–40. [PubMed: 8221091]

Kier EL, Staib LH, Davis LM, Bronen RA. MR imaging of the temporal stem: anatomic dissection tractography of the uncinate fasciculus, inferior occipitofrontal fasciculus, and Meyer's loop of the optic radiation. Am J Neuroradiol 2004;25:677–691. [PubMed: 15140705]

Kim SG, Ashe J, Hendrich K, Ellerman JM, Merkle H, Ugurbil K, Georgopoulos AP. Functional magnetic resonance imaging of motor cortex: hemispheric asymmetry and handedness. Science 1993;261:615–617. [PubMed: 8342027]

Klingberg T, Hedehus M, Temple E, Salz T, Gabrieli JD, Moseley ME, Poldrack RA. Microstructure of temporo-parietal white matter as a basis for reading ability: evidence from diffusion tensor magnetic resonance imaging. Neuron 2000;25:493–500. [PubMed: 10719902]

Kubicki M, Westin CF, Maier SE, Frumin M, Nestor PG, Salisbury DF, Kikinis R, Jolesz FA, McCarley RW, Shenton ME. Uncinate fasciculus findings in schizophrenia: a magnetic resonance diffusion tensor imaging study. Am J Psychiatry 2002;159:813–820. [PubMed: 11986136]

LaMantia AS, Rakic P. Axon overproduction and elimination in the corpus callosum of the developing rhesus monkey. J Neurosci 1990;10:2156–2175. [PubMed: 2376772]

Le Bihan D. Looking into the functional architecture of the brain with diffusion MRI. Nat Rev Neurosci 2003;4:469–480. [PubMed: 12778119]

Lenroot RK, Giedd JN. Brain development in children and adolescents: insights from anatomical magnetic resonance imaging. Neurosci Biobehav Rev 2006;30:718–729. [PubMed: 16887188] review

Luders E, Narr KL, Thompson PM, Rex DE, Jancke L, Toga AW. Hemispheric asymmetries in cortical thickness. Cereb Cortex 2006;16:1232–1238. [PubMed: 16267139]

Luders E, Narr KL, Thompson PM, Woods RP, Rex DE, Jancke L, Steinmetz H, Toga AW. Mapping cortical gray matter in the young adult brain: effects of gender. Neuroimage 2005;26:493–501. [PubMed: 15907306]

Makris N, Kennedy DN, McInerney S, Sorensen AG, Wang R, Caviness VS Jr, Pandya DN. Segmentation of subcomponents within the superior longitudinal fascicle in humans: a quantitative, in vivo, DT-MRI study. Cereb Cortex 2005;15:854–869. [PubMed: 15590909]

Makris N, Worth AJ, Sorensen AG, Papadimitriou GM, Wu O, Reese TG, Wedeen VJ, Davis TL, Stakes JW, Caviness VS, et al. Morphometry of in vivo human white matter association pathways with diffusion-weighted magnetic resonance imaging. Ann Neurol 1997;42:951–962. [PubMed: 9403488]

Matsuzawa J, Matsui M, Konishi T, Noguchi K, Gur RC, Bilker W, Miyawaki T. Age-related volumetric changes of brain gray and white matter in healthy infants and children. Cereb Cortex 2001;11:335–342. [PubMed: 11278196]

McKinstry RC, Mathur A, Miller JH, Ozcan A, Snyder AZ, Schefft GL, Almli CR, Shiran SI, Conturo TE, Neil JJ. Radial organization of developing preterm human cerebral cortex revealed by non-invasive water diffusion anisotropy MRI. Cereb Cortex 2002;12:1237–1243. [PubMed: 12427675]

Mori S, Crain BJ, Chacko VP, van Zijl PC. Three-dimensional tracking of axonal projections in the brain by magnetic resonance imaging. Ann Neurol 1999;45:265–269. [PubMed: 9989633]

Mori S, Kaufmann WE, Davatzikos C, Stieltjes B, Amodei L, Fredericksen K, Pearlson GD, Melhem ER, Solaiyappan M, Raymond GV, et al. Imaging cortical association tracts in the human brain using diffusion-tensor-based axonal tracking. Magn Reson Med 2002;47:215–223. [PubMed: 11810663]

Mori, S.; Wakana, S.; Nagae-Poetscher, LM.; van Zijl, PCM. MRI atlas of human white matter. San Diego, CA: Elsevier; 2005.

Mori S, Zhang J. Principles of diffusion tensor imaging and its applications to basic neuroscience research. Neuron 2006;51:527–539. [PubMed: 16950152]

Mukherjee P, McKinstry RC. Diffusion tensor imaging and tractography of human brain development. Neuroimaging Clin N Am 2006;16:19–43. [PubMed: 16543084]

Mukherjee P, Miller JH, Shimony JS, Conturo TE, Lee BC, Almli CR, McKinstry RC. Normal brain maturation during childhood: developmental trends characterized with diffusion-tensor MR imaging. Radiology 2001;221:349–358. [PubMed: 11687675]

Mukherjee P, Miller JH, Shimony JS, Philip JV, Nehra D, Snyder AZ, Conturo TE, Neil JJ, McKinstry RC. Diffusion-tensor MR imaging of gray and white matter development during normal human brain maturation. Am J Neuroradiol 2002;23:1445–1456. [PubMed: 12372731]

Nagy Z, Westerberg H, Klingberg T. Maturation of white matter is associated with the development of cognitive functions during childhood. J Cogn Neurosci 2004;16:1227–1233. [PubMed: 15453975]

Neil JJ, Shiran SI, McKinstry RC, Schefft GL, Snyder AZ, Almli CR, Akbudak E, Aronovitz JA, Miller JP, Lee BC, et al. Normal brain in human newborns: apparent diffusion coefficient and diffusion anisotropy measured by using diffusion tensor MR imaging. Radiology 1998;209:57–66. [PubMed: 9769812]

Nucifora PG, Verma R, Melhem ER, Gur RE, Gur RC. Leftward asymmetry in relative fiber density of the arcuate fasciculus. Neuroreport 2005;16:791–794. [PubMed: 15891571]

Park HJ, Westin CF, Kubicki M, Maier SE, Niznikiewicz M, Baer A, Frumin M, Kikinis R, Jolesz FA, McCarley RW, et al. White matter hemisphere asymmetries in healthy subjects and in schizophrenia: a diffusion tensor MRI study. Neuroimage 2004;23:213–223. [PubMed: 15325368]

Partridge SC, Mukherjee P, Berman JI, Henry RG, Miller SP, Lu Y, Glenn OA, Ferriero DM, Barkovich AJ, Vigneron DB. Tractography-based quantitation of diffusion tensor imaging parameters in white matter tracts of preterm newborns. J Magn Reson Imaging 2005;22:467–474. [PubMed: 16161075]

Paus T, Zijdenbos A, Worsley K, Collins DL, Blumenthal J, Giedd JN, Rapoport JL, Evans AC. Structural maturation of neural pathways in children and adolescents: in vivo study. Science 1999;283:1908–1911. [PubMed: 10082463]

Peled S, Gudbjartsson H, Westin CF, Kikinis R, Jolesz FA. Magnetic resonance imaging shows orientation and asymmetry of white matter fiber tracts. Brain Res 1998;780:27–33. [PubMed: 9473573]

Pierpaoli C, Jezzard P, Basser PJ, Barnett A, Di Chiro G. Diffusion tensor MR imaging of the human brain. Radiology 1996;201:637–648. [PubMed: 8939209]

Rademacher J, Burgel U, Geyer S, Schormann T, Schleicher A, Freund HJ, Zilles K. Variability and asymmetry in the human precentral motor system. A cytoarchitectonic and myeloarchitectonic brain mapping study. Brain 2001;124:2232–2258. [PubMed: 11673325]

Schmahmann, JD.; Pandya, DN. Fiber pathways of the brain. New York: Oxford; 2006.

Schmithorst VJ, Wilke M, Dardzinski BJ, Holland SK. Correlation of white matter diffusivity and anisotropy with age during childhood and adolescence: a cross-sectional diffusion-tensor MR imaging study. Radiology 2002;222:212–218. [PubMed: 11756728]

Schneider JF, Il'yasov KA, Hennig J, Martin E. Fast quantitative diffusion-tensor imaging of cerebral white matter from the neonatal period to adolescence. Neuroradiology 2004;46:258–266. [PubMed: 14999435]

Snook L, Plewes C, Beaulieu C. Voxel based versus region of interest analysis in diffusion tensor imaging of neurodevelopment. Neuroimage 2007;34:243–252. [PubMed: 17070704]

Song SK, Yoshino J, Le TQ, Lin SJ, Sun SW, Cross AH, Armstrong RC. Demyelination increases radial diffusivity in corpus callosum of mouse brain. Neuroimage 2005;26:132–140. [PubMed: 15862213]

Sowell ER, Peterson BS, Thompson PM, Welcome SE, Henkenius AL, Toga AW. Mapping cortical change across the human life span. Nat Neurosci 2003;6:309–315. [PubMed: 12548289]

Szeszko PR, Vogel J, Ashtari M, Malhotra AK, Bates J, Kane JM, Bilder RM, Frevert T, Lim K. Sex differences in frontal lobe white matter microstructure: a DTI study. Neuroreport 2003;14:2469–2473. [PubMed: 14663212]

Takahashi M, Ono J, Harada K, Maeda M, Hackney DB. Diffusional anisotropy in cranial nerves with maturation: quantitative evaluation with diffusion MR imaging in rats. Radiology 2000;216:881–885. [PubMed: 10966726]

Toga AW, Thompson PM, Sowell ER. Mapping brain maturation. Trends Neurosci 2006;29:148–159. [PubMed: 16472876]

Volpe JJ. Overview: normal and abnormal human brain development. Ment Retard Dev Disabil Res Rev 2000;6:1–5. [PubMed: 10899791]

Wakana S, Jiang H, Nagae-Poetscher LM, van Zijl PC, Mori S. Fiber tract-based atlas of human white matter anatomy. Radiology 2004;230:77–87. [PubMed: 14645885]

Yakovlev, P. Regional development of the brain in early life. Oxford: Blackwell Scientific; 1967.

Yakovlev PI, Rakic P. Patterns of decussation of bulbar pyramids and distribution of pyramidal tracts on two sides of the spinal cord. Trans Am Neurol Assoc 1966;91:366–367.

Yakovlev, PI.; LeCours, AR. The myelogenetic cycles of regional maturation of the brain. In: Minkowsky, K., editor. Regional development of the brain in early life. Oxford: Blackwell Scientific Publications; 1967. p. 3-70.

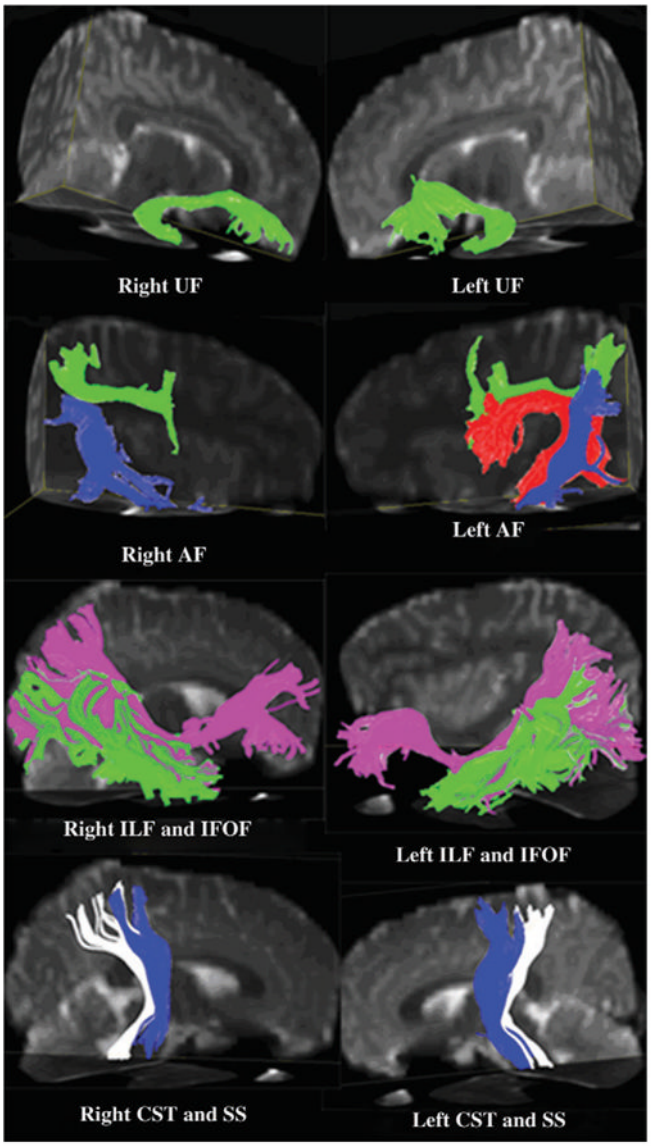

Figure 1.
Illustrative color figure displaying 3D views of reconstructed fiber tracts overlaid on B_0 (reference or no diffusion weighted) images. AF with 3 segments: FT (red fibers), FP (green fibers), and TP (blue fibers); ILF (green); IFOF (pink); CST (blue); and SS (white). Note the absent FT segment of right AF in this subject.

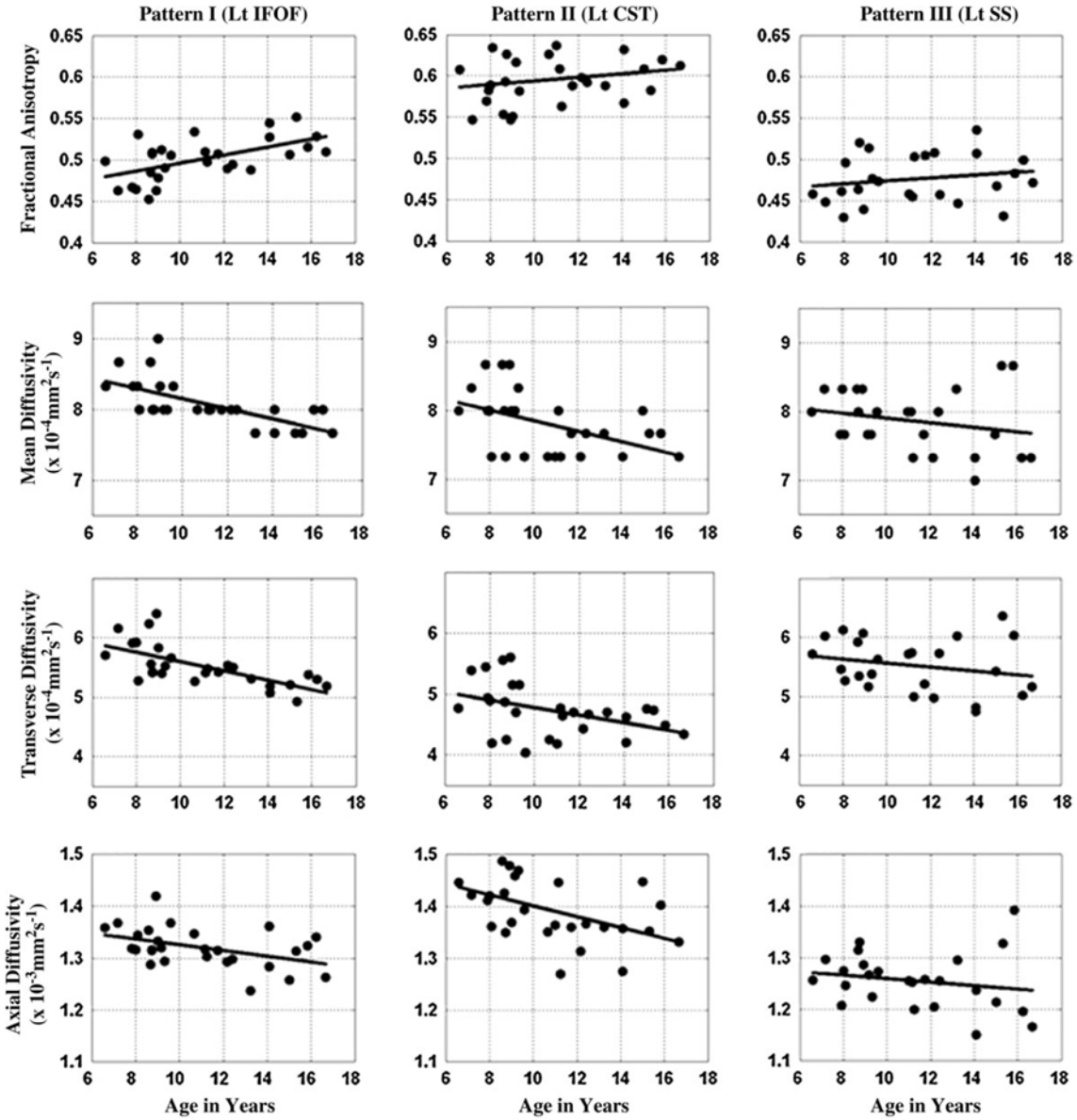

Figure 2.

Illustrative scatter plots showing various patterns of white matter maturation captured by DTT. (*A*) Pattern I: significant increase in FA with age accompanied by significant decreases in all 3 diffusivities (e.g., left IFOF). (*B*) Pattern II: significant decreases in all 3 diffusivities with age, but no significant changes in FA with age (e.g., left CST). (*C*) Pattern III: no significant changes in FA or diffusivity with age (e.g., left SS).

Table 1

Summary of the total number of subjects (boys/girls) included in the individual fiber tract studied with their mean age and SDs in years

Fiber tracts	Entire group		Boys		Girls		Boys versus girls
	N	Age ± SD	*N*	Age ± SD	*N*	Age ± SD	*P*
AF	24	11.4 ± 2.9	11	12.0 ± 3.4	13	10.9 ± 2.4	0.33
ILF	29	10.9 ± 3.0	14	11.1 ± 3.6	15	10.8 ± 2.5	0.80
IFOF	28	11.0 ± 3.0	14	11.1 ± 3.6	14	11.0 ± 2.5	0.93
UF	29	10.7 ± 2.9	13	10.7 ± 3.4	16	10.7 ± 2.4	0.93
CST	28	10.7 ± 2.9	13	10.9 ± 2.5	15	10.6 ± 3.4	0.81
SS	25	11.3 ± 3.1	11	11.6 ± 3.8	14	11.1 ± 2.5	0.66

Note: SD, standard deviation; *N*, number of participants.

Table 2

FA and mean diffusivity ($\times 10^{-3}$ mm^2 s^{-1}) of the fiber tracts studied and their correlations with age

Fiber tracts	CH	FA and age correlations			Mean diffusivity and age correlations		
		Mean ± SD	*r*	*P*<	Mean ± SD	*r*	*P*<
AF_FT	R	0.432 ± 0.064	0.16	0.45	0.705 ± 0.107	−0.18	0.40
	L	0.471 ± 0.028	0.28	0.19	0.752 ± 0.034	**−0.68**	**0.00****
AF_FP	R	0.454 ± 0.022	**0.42**	**0.04**	0.764 ± 0.042	**−0.62**	**0.00***
	L	0.437 ± 0.030	0.38	0.06	0.751 ± 0.037	**−0.67**	**0.00****
AF_TP	R	0.428 ± 0.027	0.08	0.39	0.772 ± 0.035	**−0.68**	**0.00****
	L	0.426 ± 0.029	0.25	0.24	0.763 ± 0.032	**−0.61**	**0.00***
ILF	R	0.479 ± 0.027	0.18	0.35	0.822 ± 0.037	**−0.39**	**0.04**
	L	0.490 ± 0.023	**0.48**	**0.01**	0.821 ± 0.033	**−0.57**	**0.00***
IFOF	R	0.489 ± 0.035	0.16	0.42	0.808 ± 0.036	**−0.60**	**0.00****
	L	0.500 ± 0.025	**0.57**	**0.00***	0.808 ± 0.032	**−0.66**	**0.00****
UF	R	0.424 ± 0.023	**0.41**	**0.03**	0. 807 ± 0.034	**−0.69**	**0.00*****
	L	0.432 ± 0.027	**0.49**	**0.01**	0.803 ± 0.034	**−0.66**	**0.00****
CST	R	0.579 ± 0.030	**0.50**	**0.01**	0.782 ± 0.036	−0.35	0.07
	L	0.595 ± 0.029	0.21	0.29	0.780 ± 0.045	**−0.49**	**0.01**
SS	R	0.473 ± 0.022	0.18	0.39	0.792 ± 0.048	−0.24	0.24
	L	0.476 ± 0.029	0.19	0.37	0. 787 ± 0.045	−0.23	0.27

Note: CH, cerebral hemisphere; R, right; L, left; and *r*, Pearson product-moment correlation coefficient; SD, standard deviation. The values of r and P are given in boldface whenever the corresponding P <0.05.

* *P* <0.005,

** *P* <0.0005,

*** *P* <0.00005.

Table 3

Transverse diffusivity ($\times 10^{-3}$ mm^2 s^{-1}) and axial diffusivity ($\times 10^{-3}$ mm^2 s^{-1}) of the fiber tracts studied and their correlations with age

Fiber tracts	CH	Transverse diffusivity and age correlations			Axial diffusivity and age correlations		
		Mean ± SD	*r*	*P*<	Mean ± SD	*r*	*P*<
AF_FT	R	0.512 ± 0.059	−0.33	0.12	1.091 ± 0.021	−0.09	0.67
	L	0.531 ± 0.034	**−0.61**	**0.00***	1.196 ± 0.049	**−0.58**	**0.00***
AF_FP	R	0.548 ± 0.038	**−0.62**	**0.00***	1.194 ± 0.055	**−0.55**	**0.00***
	L	0.547 ± 0.039	**−0.62**	**0.00***	1.156 ± 0.046	**−0.55**	**0.00***
AF_TP	R	0.568 ± 0.037	**−0.55**	**0.01**	1.179 ± 0.041	**−0.73**	**0.00*****
	L	0.562 ± 0.034	**−0.53**	**0.01**	1.162 ± 0.041	**−0.52**	**0.01**
ILF	R	0.574 ± 0.035	−0.36	0.06	1.315 ± 0.056	−0.30	0.11
	L	0.567 ± 0.032	**−0.61**	**0.00****	1.327 ± 0.044	−0.36	0.06
IFOF	R	0.559 ± 0.035	**−0.52**	**0.00***	1.306 ± 0.064	**−0.42**	**0.03**
	L	0.552 ± 0.035	**−0.67**	**0.00****	1.320 ± 0.038	**−0.44**	**0.02**
UF	R	1.596 ± 0.035	**−0.64**	**0.00****	1.228 ± 0.038	**−0.64**	**0.00***
	L	1.589 ± 0.037	**−0.64**	**0.00****	1.232 ± 0.037	**−0.51**	**0.00***
CST	R	0.485 ± 0.035	**−0.50**	**0.01**	1.376 ± 0.058	−0.03	0.88
	L	0.473 ± 0.043	**−0.41**	**0.03**	1.392 ± 0.061	**−0.49**	**0.01**
SS	R	0.557 ± 0.041	−0.26	0.22	1.261 ± 0.070	−0.20	0.33
	L	0.552 ± 0.045	−0.23	0.27	1.255 ± 0.054	−0.19	0.35

Note: CH, cerebral hemisphere; R, right; L, left; *r*, Pearson product-moment correlation coefficient; SD, standard deviation. The values of r and P are given in boldface whenever the corresponding P <0.05.

* *P* <0.005,

** *P* <0.0005,

*** *P* <0.00005.